# Dioxygen Activation at Non-Heme Iron: Insights from Rapid Kinetic Studies

IVAN V. KORENDOVYCH, SERGEY V. KRYATOV, AND ELENA V. RYBAK-AKIMOVA*

*Department of Chemistry, Tufts University, Medford, Massachusetts 02155*

## ABSTRACT

One of the common biochemical pathways of binding and activation of dioxygen involves non-heme iron centers. The enzyme cycles usually start with an iron(II) or diiron(II) state and traverse via several intermediates (detected or postulated) such as (di)iron(III)–superoxo, (di)iron(III)–(hydro)peroxo, iron(III)iron(IV)–oxo, and (di)iron(IV)–oxo species, some of which are responsible for substrate oxidation. In this Account, we present results of kinetic and mechanistic studies of dioxygen binding and activation reactions of model inorganic iron compounds. The number of iron centers, their coordination number, and the steric and electronic properties of the ligands were varied in several series of well-characterized complexes that provided reactive manifolds modeling the function of native non-heme iron enzymes. Time-resolved cryogenic stopped-flow spectrophotometry permitted the identification of kinetically competent intermediates in these systems. Inner-sphere mechanisms dominated the chemistry of dioxygen binding, intermediate transformations, and substrate oxidation as most of these processes were controlled by the rates of ligand substitution at the iron centers.
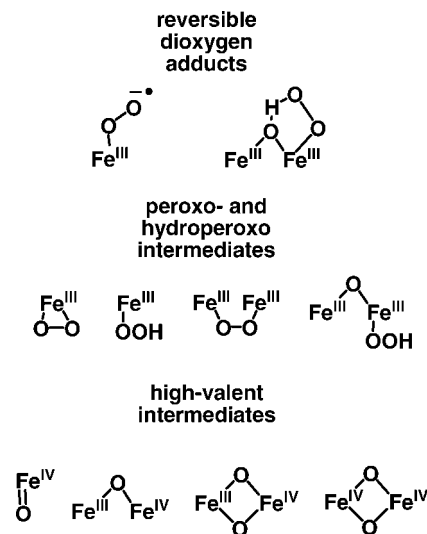
## Introduction

Aerobic organisms have developed numerous metal-based reactions for dioxygen binding and activation for biological energy production and for efficient and selective organic substrate oxidations. Iron is most commonly used in oxidative metalloenzymes, and iron–peroxo or high-valent iron–oxo intermediates are involved in oxygen

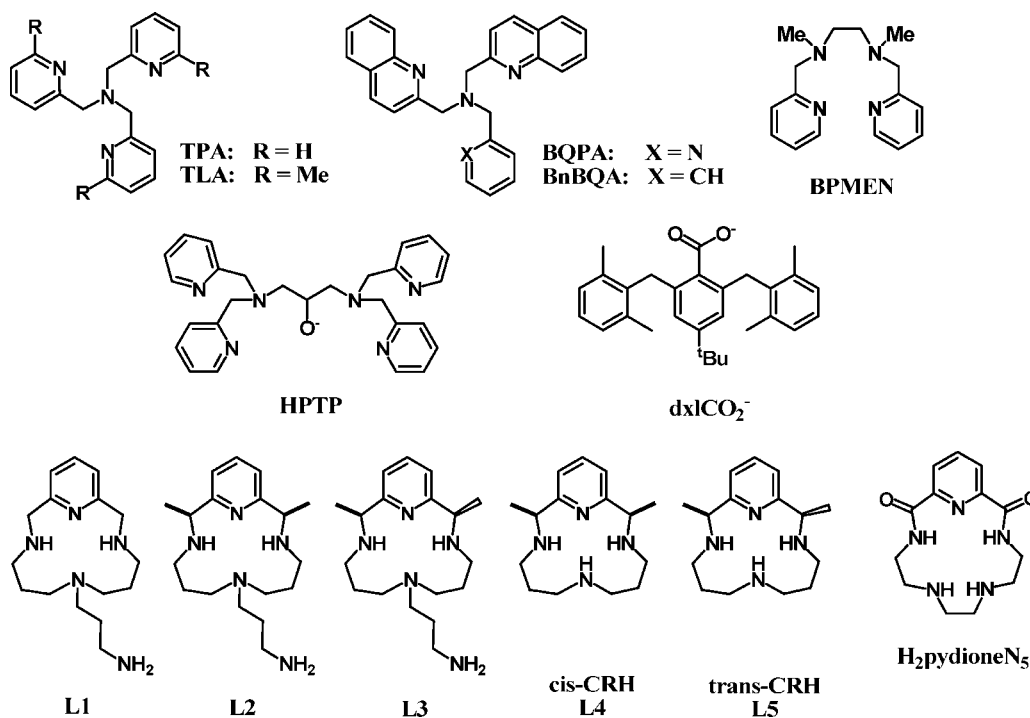**Scheme 1.  Intermediates Observed in Non-Heme Iron Proteins and Model Complexes**



activation with iron oxidases and oxygenases. In contrast, free radical pathways (Fenton chemistry) are common for iron salts and traditional inorganic iron compounds, producing HO• radicals as active but unselective oxidants. Mimicking enzymelike "hydroxyl-radical free" oxidations with synthetic iron complexes requires a detailed understanding of the oxidation mechanisms and reproduction of their key features. Identifying kinetically competent, reactive intermediates is critical in designing metalloenzyme functional models and ultimately in synthesizing useful, selective, and efficient catalysts utilizing dioxygen and hydrogen peroxide as terminal oxidants.

Our group focuses on the detailed characterization of the formation and reactivity of various non-heme iron–peroxo and iron–oxo intermediates (Scheme 1). Previous synthetic, spectroscopic, structural, and computational studies established the chemical nature of these iron-based intermediates[1] and provided necessary background information for interpreting mechanistic data. Available mechanistic insights were traditionally obtained by analysis of product distribution in catalytic or stoichiometric substrate oxidations, combined with quantum chemical calculations on iron–peroxo and high-valent iron–oxo complexes.[1] These studies suggest that the structure, oxidation state, spin state, and protonation state of metal-based intermediates all influence their reactivity. However, the reactivity profiles of these intermediates, which define their intrinsic selectivity with respect to oxidation of various substrates, were rarely studied in direct experiments.[2] The cryogenic stopped-flow technique, which detects "in real time", on a millisecond time scale, rapidly accumulating and decaying intermediates (often unstable at room temperature), allows us to uncover structure–reactivity correlations for individual reaction steps involved in oxygen and peroxide activation. Rapid mixing

Ivan V. Korendovych received his B.S. and M.S. degrees from National Taras Shevchenko University (Kiev, Ukraine). In 2006, he received his Ph.D. degree from Tufts University working on mechanistic aspects of oxygen activation and anion recognition in the lab of Professor Rybak-Akimova. At present, he is a postdoctoral fellow at the University of Pennsylvania (Philadelphia, PA) in the group of William DeGrado.

Sergey V. Kryatov received a Diploma in Chemistry (B.S./M.S.) from Kiev State University (presently National Taras Shevchenko University) in 1991 and a Ph.D. degree from the Institute of Physical Chemistry of the Ukrainian Academy of Sciences in 1997. In 1998–2005, he worked as a research associate in the group of Elena Rybak-Akimova at Tufts University studying kinetics and mechanisms of small molecule binding and activation by metal complexes in solution. Currently, he is a lecturer in chemistry at Tufts University.

Elena V. Rybak-Akimova received her M.S. from Kiev State University and her Ph.D. from the Institute of Physical Chemistry of the Ukrainian Academy of Sciences (with Konstantin B. Yatsimirskii). She then spent several years (1993–1997) at the University of Kansas (Lawrence, KS) as a postdoctoral associate with Daryle H. Busch. In 1997, she joined the faculty of Tufts University, where she is presently an Associate Professor. Her current research focuses on understanding the mechanisms of small molecule (O₂ and N₂) activation with biomimetic transition metal complexes and designing selective metal-containing receptors, reagents, and catalysts.

* Corresponding author.

**Scheme 2. Ligands Employed in the Studies of Oxygen Activation**

TPA: R = H
TLA: R = Me

BQPA: X = N
BnBQA: X = CH

BPMEN

HPTP

dxlCO$_2^-$

L1  L2  L3

cis-CRH L4    trans-CRH L5

H$_2$pydioneN$_5$

of reactants occurs in a stainless steel cell immersed in a cooling bath maintained at temperatures down to −90 °C inside a Dewar flask with liquid nitrogen (Figure 1). This technique provides kinetic and mechanistic insights ultimately applicable to the rational design of selective oxidation catalysts.

In this Account, we summarize the results of kinetic and mechanistic studies of (1) O$_2$ coordination to diiron(II) centers yielding diiron(III)–peroxo intermediates, (2) generation of diiron(III)–peroxo intermediates from mononuclear iron(II) complexes and O$_2$, (3) reaction of di-

**Scheme 3. Modeling the Dioxygen Activating Cycle of RNR R2[5]**

L = TLA
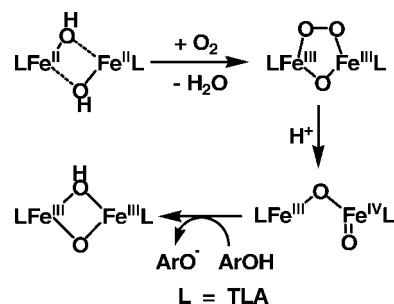
iron(III)–peroxo species with substrates, (4) "peroxide shunt" pathways generating diiron(III)–hydroperoxo and Fe(III)Fe(IV) intermediates from diiron(III) precursors and H$_2$O$_2$, and (5) olefin epoxidation and aromatic hydroxylation with H$_2$O$_2$. In most of these studies, various aminopyridine ligands were utilized, along with sterically hindered carboxylates for comparison (Scheme 2). The rich chemistry of iron complexes with the aminopyridine tripodal ligand TPA and its derivatives, extensively studied by L. Que and co-workers,[3,4] yielded spectroscopically and even structurally characterized iron(III)–peroxo and high-valent iron(IV)–oxo intermediates in both mononuclear and dinuclear systems, thus enabling systematic studies of rates and mechanisms of their formation and subsequent reactions with substrates.

## Reactions of Diiron(II) Complexes with O$_2$

Oxygen activation with non-heme diiron enzymes involves the electronically complementary reaction (Fe$^{II}$)$_2$ + O$_2$ → (Fe$^{III}$)$_2$($\mu$-O$_2^{2-}$), which generates no radicals, producing instead a potentially reactive peroxo intermediate. Subsequent reactions may lead to substrate oxidation. For
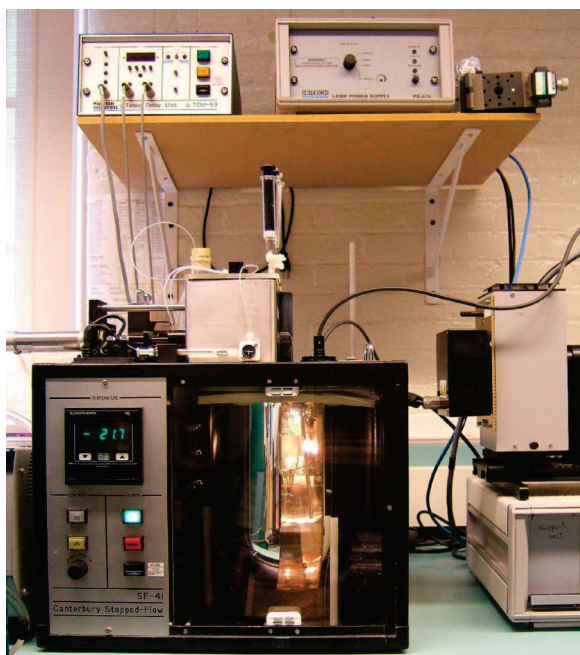


**FIGURE 1.** Cryogenic stopped-flow instrument (SF-43 from Hi-Tech Scientific).

**Table 1. Kinetic Parameters for Reactions of Diiron(II) Complexes with Dioxygen**

| complex | solvent | $T$ range (°C) | $k(-40\ °C)$ ($M^{-1}\ s^{-1}$) | $\Delta H^{\ddagger}$ (kJ/mol) | $\Delta S^{\ddagger}$ ($J\ K^{-1}\ mol^{-1}$) | ref |
|---|---|---|---|---|---|---|
| $[Fe_2(HPTP)(O_2CPh)]^{2+}$ | MeCN | −40 to 0 | 7300 | 15.8(4) | −101(10) | 8 |
| $[Fe_2(HPTP)(O_2CPh)]^{2+}$ | MeCN/DMSO (9:1, v/v) | −40 to 0 | 2800 | 8.0(3) | −143(10) | 8 |
| $[Fe_2(HPTP)(O_2CPh)]^{2+}$ | $CH_2Cl_2$ | −80 to 0 | 67 | 16.7(2) | −132(8) | 8 |
| $[Fe_2(dxlCO_2)_4(Py)_2]$ | $CH_2Cl_2$ | −80 to −30 | 215 | 4.7(5) | −178(10) | 9, 10 |
| $[Fe_2(dxlCO_2)_4(MeIm)_2]$ | $CH_2Cl_2$ | −80 to −30 | 300 | 10.1(10) | −153(10) | 9, 10 |
| $[Fe_2(dxlCO_2)_4(THF)_2]$ | $CH_2Cl_2$ | −80 to −30 | 3.20 | 14(1) | −135(10) | 9, 10 |
| $[Fe_2(OH)_2(TLA)_2]^{2+}$ | $CH_2Cl_2$ | −80 to −40 | 0.67 | 17(2) | −175(10) | 9, 10 |
| $[Fe_2(OH)_2(TLA)_2]^{2+}$ | MeCN | −40 to −5 | 1.94 | 16(2) | −167(10) | 7 |
| $[Fe_2(OH)_2(TPA)_2]^{2+}$ | $CH_2Cl_2$ | −40 to −15 | 12 | 30(4) | −94(10) | 7 |
| $[Fe_2(OH)_2(BQPA)_2]^{2+}$ | $CH_2Cl_2$ | −40 to −15 | 3.2 | 36(4) | −80(10) | 7 |
| $[Fe_2(OH)_2(BQPA)_2]^{2+}$ | $CH_2Cl_2/NEt_3$ | −70 to −40 | 2.6 | 36(4) | −81(10) | 7 |
| $[Fe_2(OH)_2(BnBQA)_2]^{2+}$ | MeCN | −65 to −25 | 2670 | 16(2) | −108(10) | 7 |
| $[Fe_2(OH)(OH_2)(TPA)_2]^{3+}$ | $CH_2Cl_2$ | −30 to 20 | 0.32 | 19(2) | −170(10) | 11 |

example, a dihydroxo-bridged complex $[Fe^{II}_2$-$(\mu$-OH$)_2(TLA)_2]^{2+}$ mimicked the catalytic cycle of ribonucleotide reductase (Scheme 3): the initially formed metastable peroxo intermediate could undergo acid-promoted conversion to an $Fe^{III}Fe^{IV}$ species capable of oxidizing phenols.[5] Significant steric crowding about iron sites, created by methyl-substituted pyridine donors, resulted in the relative stabilization of the intermediates. In this section, we discuss dioxygen binding to $[Fe^{II}_2(\mu$-OH$)_2(TLA)_2]^{2+}$ and analogous complexes with TPA, BQPA, and BnBQA (Scheme 1); the reactions of Fe(III)Fe(IV) species with substrates will be addressed later.

Dinuclear complexes $[Fe^{II}_2(\mu$-OH$)_2(L)_2]^{2+}$ (L = TLA, TPA, BQPA, and BnBQA) react with $O_2$.[5–7] In selected solvents, the oxygenation of complexes with TLA, BQPA, and BnBQA at low temperatures gives diiron(III)–peroxo species; the yield of these species could often be increased in the presence of organic bases. Under other conditions, the oxo-bridged iron(III) oligomers $[Fe^{III}_n(O)_n(L)_n]^{n+}$ (n = 2 or 3) formed.[7]

In all cases, the reaction was first-order in both diiron(II) complex and $O_2$ and had a low activation enthalpy and a strongly negative activation entropy (Table 1), in agreement with expectations for an associative process.[6,7] Both extrusion of water from the diiron–bishydroxo core and O–H bond breaking (hydrogen atom transfer or proton-coupled electron transfer) are post-rate-limiting steps, because oxygenation rates did not depend on the concentration of $H_2O$ or $D_2O$.[6]

Kinetic evidence points to $O_2$ coordination to one of the iron(II) centers in $Fe_2(OH)_2$ cores as being the rate-limiting step in the overall oxygenation process and implies the initial formation of a diiron–superoxo intermediate (Scheme 4). Indeed, such an intermediate was recently observed in the oxygenation of $[Fe_2(OH)_2(TLA)_2]^{2+}$ at a low temperature (−80 °C),[12] and the activation parameters of its formation were essentially identical to the activation parameters of the formation of a more stable $\mu$-1,2-peroxo intermediate (Scheme 4 and Table 1).

Binding of the $O_2$ molecule to the diiron(II) core is limited by the rates of ligand substitution rather than by electron-transfer rates. An outer-sphere one-electron transfer is unlikely, because the potential for the $O_2/O_2^-$ redox pair in organic solvents is 1 V more negative than those

**Scheme 4**

L = TPA, TLA, BnBQA, BQPA

$[Fe^{II}_2(OH)(OH)]^{2+}$
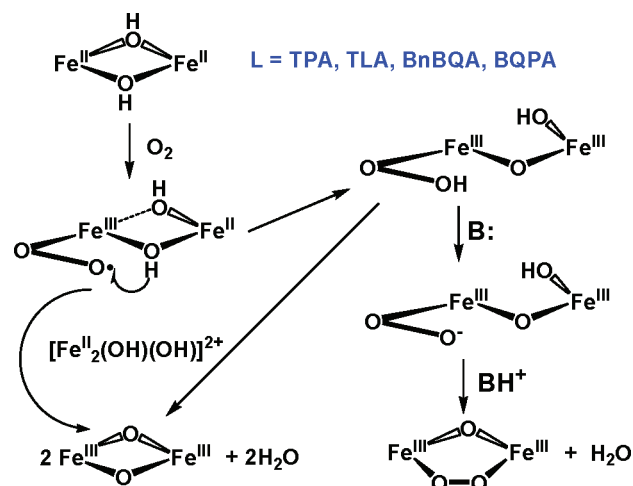
determined for the $Fe^{II}Fe^{III}/Fe^{II}Fe^{II}$ redox pairs.[7] Furthermore, the oxygenation rates for a series of diiron(II) complexes (Table 1) do not correlate with their redox potentials.[7] Instead, the oxygenation rates correlate best with the length of the weakest Fe–donor atom bond in the diiron(II) complex, suggesting that dissociation of one (or more) of the donor atoms initially bound to iron(II) is involved in $O_2$ binding.

Extreme steric hindrance about iron coordination sites in complexes with TLA protects the peroxo intermediate from oxidative decomposition but simultaneously makes iron(II) centers much less accessible to even a small incoming $O_2$ molecule, resulting in slow oxygenation ($t_{1/2} \approx 30$ min at −40 °C).[6] A decrease in the steric bulk of the tetradentate ligands failed to significantly improve oxygenation rates, presumably because of a more "compact" and symmetric structure of the $Fe^{II}_2(OH)_2$ cores: the less negative activation entropies for these complexes were offset by the higher activation enthalpies (Table 1) required to break the shorter Fe–O(H) and/or Fe–N(py) bonds in the course of oxygen binding.

Understanding the mechanism of associative, entropically controlled oxygen binding to the six-coordinate $Fe^{II}_2(OH)_2$ complexes allowed us to design the systems that undergo rapid oxygenation. In agreement with predicted facile oxygenation in coordinatively unsaturated iron(II) complexes featuring a vacant or labile site, a remarkable 1000-fold acceleration of dioxygen binding to
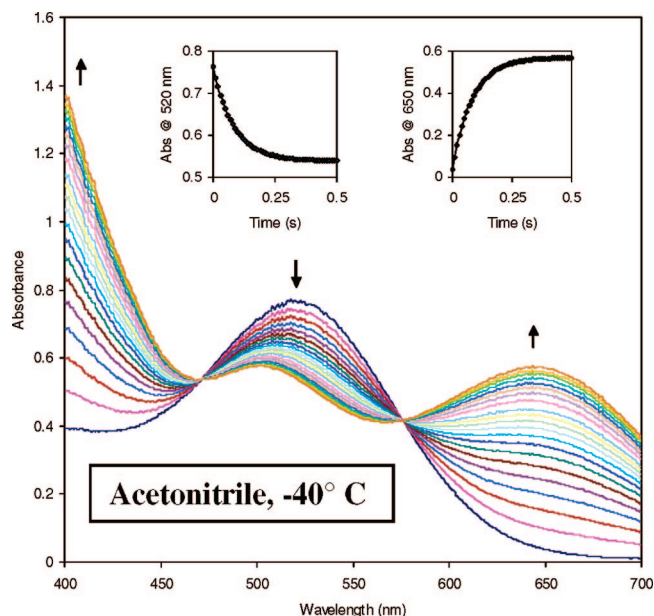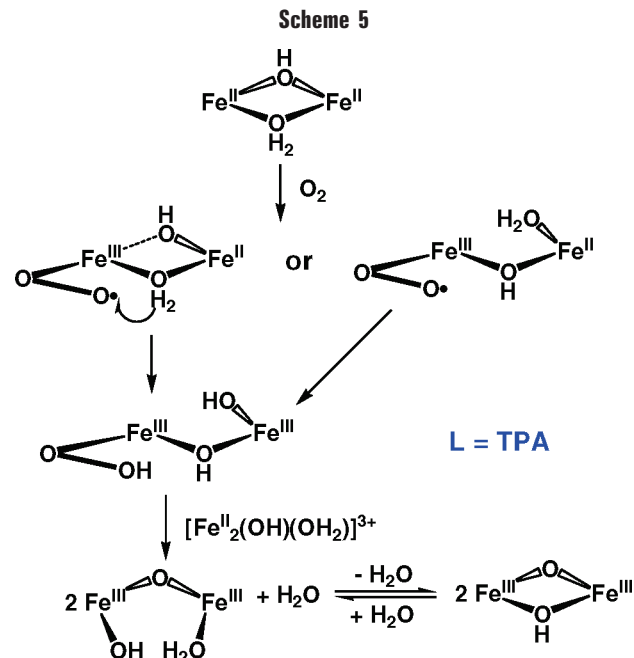
FIGURE 2. Time-resolved UV–vis spectra during the reaction of [Fe$_2$(OH)$_2$(BnBQA)$_2$]$^{2+}$ with O$_2$.

[Fe$^{II}$$_2$(OH)$_2$(BQPA)$_2$]$^{2+}$ was accomplished by replacing one pyridine arm in BQPA with a noncoordinating benzyl group in BnBQA (Figure 2).[7]
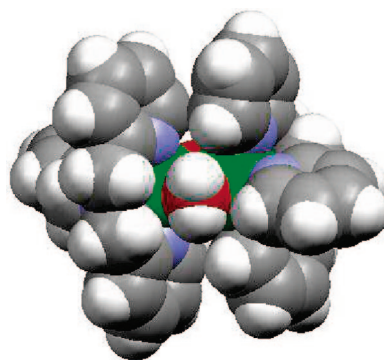
The addition of a noncoordinating base [e.g., triethylamine, isopropylethylamine, 1,4-diazabicyclo[2.2.2]octane (DABCO), 1,8-diazabicyclo[4.3.0]non-5-ene (DBU), or *N,N,N′,N′*-tetramethylguanidine] does not influence the oxygenation rate but, in some cases {especially for [Fe$_2$(OH)$_2$(BQPA)$_2$]$^{2+}$}, increases substantially the yield of peroxo intermediates, revealing the involvement of a proton-sensitive step that controls the reactivity of the initial O$_2$ adduct (Scheme 4). In the absence of base, the intermediate O$_2$ adduct can oxidize the residual diiron(II) complex, yielding oxo-bridged diiron(III) products.[7] Alternatively, it can rearrange into a potentially reactive diiron(III)–hydroperoxo intermediate. In the presence of base, deprotonation the hydroxo bridge in the diiron–O$_2$ adduct or the hydroperoxo ligand in diiron(III)–hydroperoxo species is facilitated, promoting formation of a diiron(III)–peroxo complex.[6] Electrophilically activated diiron(III)–hydroperoxo species may be useful in substrate oxidations if competing, unproductive reactions with the starting Fe(II) species can be prevented.

To further study the effects of protonation and deprotonation on oxygenation reactions, we investigated a novel diiron(II) diamond core complex with bridging water and hydroxide groups,[11] a motif often present in various forms of soluble methane monooxygenase.[13] The crystallographically characterized complex [Fe$_2$(OH)(OH$_2$)(TPA)$_2$]$^{3+}$ is stable both in nonpolar solvents and in the solid state. In contrast to the effects of added base, protonation of one hydroxo bridge in [Fe$_2$(OH)$_2$(TPA)$_2$]$^{2+}$ did not stabilize peroxide complexes in oxygenation, presumably due to the increased reactivity of the protonated hydroperoxo intermediate with another molecule of diiron(II) complex, yielding an oxo-hydroxo–diiron(III) product (Scheme 5).
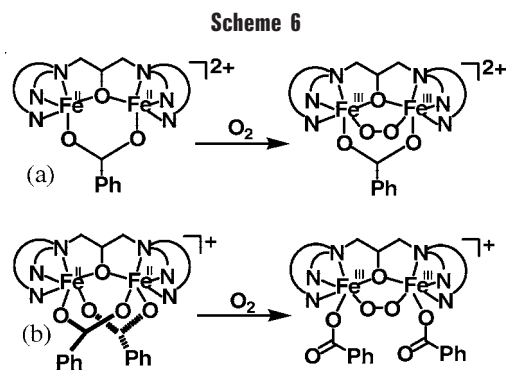
**Scheme 5**



[Fe$_2$(OH)(OH$_2$)(TPA)$_2$]$^{3+}$ has an oxidation potential ca. 1 V higher than that of its bis-hydroxo-bridged analogue, [Fe$_2$(OH)$_2$(TPA)$_2$]$^{2+}$. Such a drastic difference in redox potential between these complexes is accompanied by an only moderate difference in dioxygen reactivity, indicating that inner-sphere dioxygen coordination is a rate-limiting event (an alternative outer-sphere electron transfer pathway would result in a 10$^8$-fold difference in rates).[11] The kinetic parameters [small $\Delta H^\ddagger$ and large negative $\Delta S^\ddagger$ (Table 1)] strongly support an associative, entropically controlled mechanism for oxygenation of the hydroxo-aqua-bridged diiron(II) core, analogous to the mechanism of binding of O$_2$ to bis-hydroxo-bridged complexes.

The Fe–OH$_2$ bonds in [Fe$_2$($\mu$-OH)($\mu$-H$_2$O)(TPA)$_2$]$^{3+}$ are longer than the Fe–O(H) bonds in its bis-hydroxo-bridged analogue. This weakening of the Fe$_2$O$_2$ core upon protonation of the hydroxo bridge may result in facile oxygenation, an effect observed recently for diiron complexes with carboxylate-rich ligands.[14] In the case of TPA-supported complexes, the activation barrier for binding of O$_2$ to [Fe$_2$($\mu$-OH)($\mu$-H$_2$O)(TPA)$_2$]$^{3+}$ is indeed lower than that for [Fe$_2$($\mu$-OH)$_2$(TPA)$_2$]$^{2+}$ (Table 1), but enthalpy–entropy compensation results in slightly slower oxygenation



FIGURE 3. Space filling representation of the X-Ray structure of [Fe$_2$($\mu$-OH)($\mu$-H$_2$O)(TPA)$_2$]$^{3+}$.

**Scheme 6**





FIGURE 4. Time-resolved UV–vis spectra of the formation of $[Fe_2(O_2)(HPTP)(BzO)]^{2+}$ (a) and the corresponding kinetic traces (both in the presence and in the absence of $PPh_3$) (b).
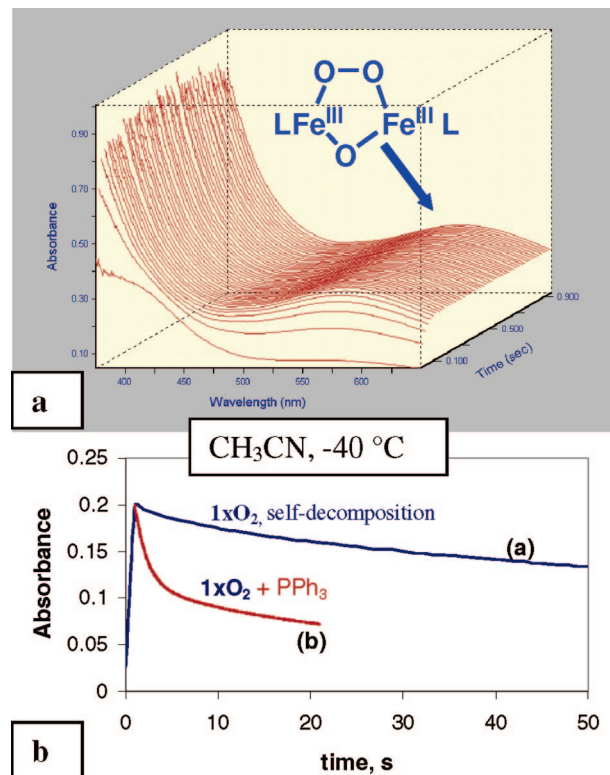
of hydroxo-aqua species. Rate-limiting binding of $O_2$ to the first iron center in $[Fe_2(\mu\text{-}OH)(\mu\text{-}H_2O)(TPA)_2]^{3+}$ likely involves breaking the Fe–$OH_2$ bond rather than the Fe–N(py) bond, consistent with an unfavorable activation entropy. Access to the iron centers, shielded by bulky TPA ligands, is limited in the starting complex (Figure 3) and is hardly improved by breaking the aqua bridge inside the core.

The mechanistic studies and structure–reactivity correlations established for diiron–bis-hydroxo-bridged complexes suggest a strategy for facile oxygenation of diiron(II) cores: a vacant or labile site at the metal center should be available. This strategy also works well for other classes of diiron(II) complexes, such as alkoxo-bridged complexes with dinucleating aminopyridine ligands, and complexes with sterically hindered carboxylates.

The oxygenation of diiron(II) complexes with a dinucleating ligand HPTP (Scheme 1) is much faster than the oxygenation of the six-coordinate, sterically hindered complex $[Fe_2(OH)_2(TLA)_2]^{2+}$. The ligand HPTP provides three nitrogen donors per iron, and two additional coordination sites are occupied by bridging oxygen atoms (from the alkoxo and carboxylato groups). The sixth coordination site remains available for facile small ligand binding. The peroxo intermediates in HPTP systems are known to be greatly stabilized by coordination of oxygen donors, such as DMSO, phosphine oxides, or an additional carboxylate anion.[8] We found that coordination of a labile monodentate ligand (such as DMSO) in the sixth position does not significantly retard the oxygenation step, but coordination of a second carboxylate anion (Scheme 6b) slows $O_2$ binding by a factor of 10. The reactions of diiron(II)–HPTP complexes with $O_2$ were low-barrier, entropically controlled, second-order processes.[8]

Oxygenation of paddle-wheel complexes with the sterically hindered carboxylate ligand $dxlCO_2^-$ at low temperatures also cleanly produced an intermediate containing coordinated $O_2$ (Scheme 7).[9,10] The nature of capping ligands L (THF, pyridine, or 1-methylimidazole) exerted little effect on the kinetic parameters of dioxygen binding at a vacant iron site, which proceeded in an isokinetic regime, suggesting a similar rate-determining step.[10] Rapid dioxygen binding (Table 1) to these five-coordinate iron(II) center(s) again occurs in a bimolecular associative process, as evidenced by small activation enthalpies and large negative activation entropies. These mechanistic features
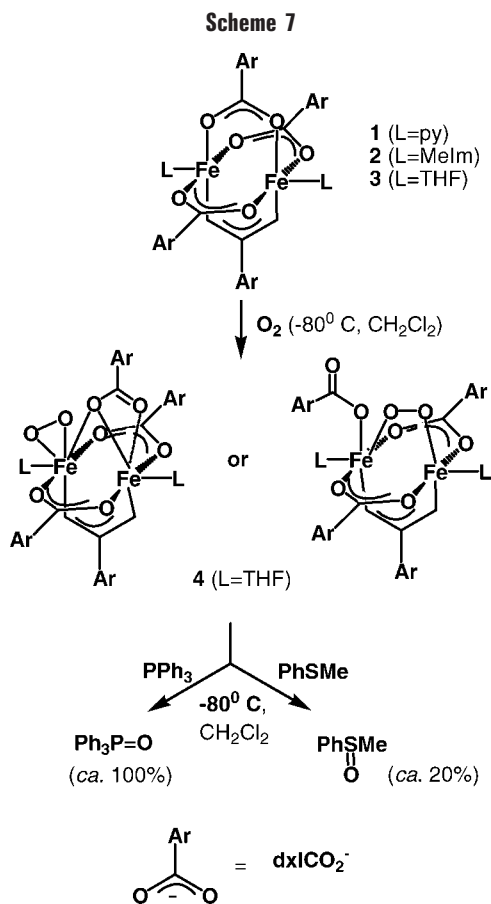
are shared by several classes of diiron(II) complexes studied in our laboratory.

## Reactions of Mononuclear Iron Complexes with $O_2$

Diiron(III)–peroxo intermediates can be generated from mononuclear or dinuclear iron(II) complexes. Mechanistically, the first step of oxygen coordination to an iron(II) center is usually rate-limiting for dinuclear complexes; geometric proximity and electronic coupling of the two irons account for a rapid decomposition of the initially formed diiron–superoxo complexes into more stable $\mu$-1,2-peroxo species. Oxygenation of mononuclear complexes is different: the initially formed superoxo adduct may attack a second molecule of the Fe(II) complex in a slower, bimolecular process. Therefore, mononuclear complexes provide a better chance to study the mechanism of the second iron–oxygen bond formation step. Excessive steric bulk, which favors mononuclear iron–dioxygen adducts, prevents formation of peroxo–dimeric species and therefore was avoided in our studies.
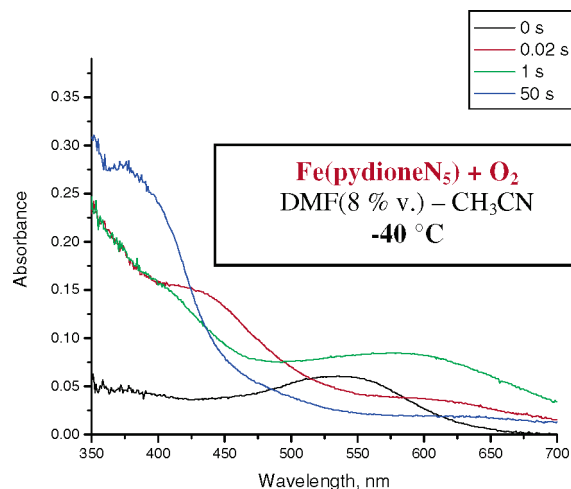
To construct a system to generate intermediates of biological relevance, we have chosen the amide-containing macrocycle $H_2pydioneN_5$ (Scheme 2).[15] Unlike the majority of strongly $\sigma$-donating electron-rich amide-containing ligands that form low-spin complexes, pentaaza macrocycle $H_2pydioneN_5$ forms exclusively high-spin iron(II) and iron(III) complexes stabilized by the pseudo-5-fold symmetry of the relatively large, rigid ring.[15,16] We have obtained and crystallographically char-

**Scheme 7**



**1** (L=py)
**2** (L=MeIm)
**3** (L=THF)

O$_2$ (-80$^0$ C, CH$_2$Cl$_2$)

**4** (L=THF)

PPh$_3$          PhSMe

-80$^0$ C,
CH$_2$Cl$_2$

Ph$_3$P=O          PhSMe
(*ca.* 100%)          O     (*ca.* 20%)

Ar
O — C       =   **dxlCO$_2$$^-$**
O — O



**FIGURE 5.** UV–vis spectra of the reaction mixture during the reaction of Fe(pydioneN$_5$) with O$_2$: black for the starting Fe(pydioneN$_5$), red for the iron–superoxo species, green for the diiron–peroxo species, and blue fof the decomposition product.

acterized both mono- and dideprotonated versions of the iron(II) complex in the solid state and shown that the deprotonation state persists in DMSO solvent. The mono-deprotonated complex features an intramolecular source of proton(s) that modulates oxygenation chemistry.

Oxygenation of the dideprotonated complex of Fe(II), Fe(pydioneN$_5$), in aprotic solvents proceeds via a path analogous to that of iron(II) porphyrins: via iron(III)–superoxo and diiron(III)–peroxo species, as evidenced by spectral changes observed during the reaction (Figure 5). The reaction is second-order in the iron(II) complex and shows an inverse dependence of reaction rate on dioxygen concentration. The presence of 1-methylimidazole stabilizes the diiron–peroxo intermediate: the half-life increases by 2 orders of magnitude.

The reaction of Fe(pydioneN$_5$) with dioxygen in methanol is distinctly different: it is first-order in both iron(II) complex and dioxygen, with no spectroscopically observed intermediate. Similar behavior was observed for the monodeprotonated complex Fe(HpydioneN$_5$) in various
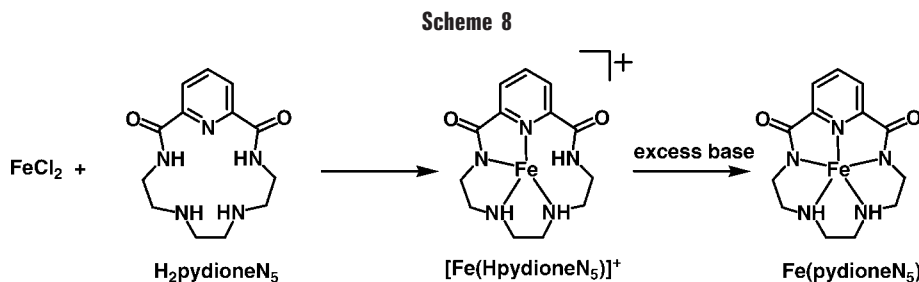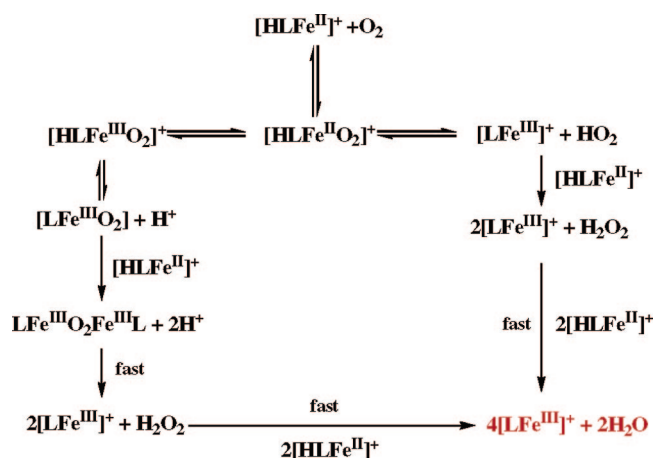
solvents. The presence of an accessible proton in the vicinity of the reaction center or from the solvent altered the oxygenation pathway in these macrocyclic systems (Scheme 9).

The reactions of Fe(pydioneN$_5$) with O$_2$ (very rapid initial coordination followed by bimolecular rapid formation of a diiron–peroxo intermediate) are similar to those of porphyrins. The extra donor atom in the pentadentate, sterically unhindered "porphyrin analogue" H$_2$pydioneN$_5$ does not prevent rapid generation of diiron(III)–peroxo intermediates, which can therefore be readily accessed from the mononuclear precursors.
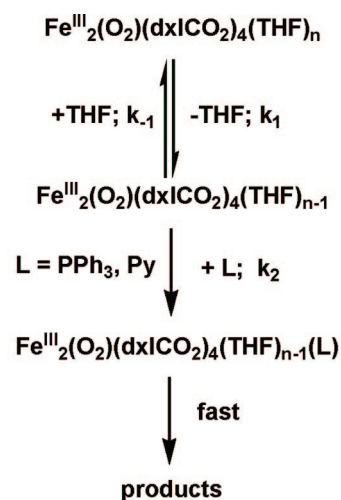
## Reactivity of Diiron–Peroxo Intermediates

The ability of diiron(III)–peroxo intermediates to oxidize substrates in formally two-electron processes was established for some enzymatic oxidations [e.g., oxidations of olefins, ethers, or nitroalkanes with Fe$_2$(O$_2$) intermediates of methane monooxygenase, or oxidations of aromatic substrates with Fe$_2$(O$_2$) adducts of toluene monooxygenase and related enzymes].[17] However, relatively stable diiron(III)–peroxo species in synthetic model systems did not transfer an oxygen atom to substrates but demonstrated nucleophilic reactivity instead.[2,18] We hypothesized that less stable diiron–O$_2$ adducts can oxidize external substrates. The reactivity of short-lived, metastable intermediates was studied in double-mixing stopped-flow experiments. Diiron(II) complex was mixed with O$_2$ at low temperatures, and dioxygen adduct accumulated. A sub-

**Scheme 8**



FeCl$_2$ +

**H$_2$pydioneN$_5$**     →     **[Fe(HpydioneN$_5$)]$^+$**     excess base →     **Fe(pydioneN$_5$)**

**Scheme 9. Oxygenation of [Fe(HpydioneN$_5$)]$^+$**

$$[HLFe^{II}]^+ + O_2$$

$$[HLFe^{III}O_2]^+ \rightleftharpoons [HLFe^{II}O_2]^+ \rightleftharpoons [LFe^{III}]^+ + HO_2$$

$$[LFe^{III}O_2] + H^+ \qquad\qquad [HLFe^{II}]^+$$

$$[HLFe^{II}]^+ \qquad\qquad 2[LFe^{III}]^+ + H_2O_2$$

$$LFe^{III}O_2Fe^{III}L + 2H^+$$

$$\downarrow \text{fast} \qquad\qquad \text{fast} \quad 2[HLFe^{II}]^+$$

$$2[LFe^{III}]^+ + H_2O_2 \xrightarrow[2[HLFe^{II}]^+]{\text{fast}} 4[LFe^{III}]^+ + 2H_2O$$

**Scheme 10**

$$Fe^{III}_2(O_2)(dxlCO_2)_4(THF)_n$$

$$+THF; k_{-1} \updownarrow -THF; k_1$$

$$Fe^{III}_2(O_2)(dxlCO_2)_4(THF)_{n-1}$$

$$L = PPh_3, Py \downarrow +L; k_2$$

$$Fe^{III}_2(O_2)(dxlCO_2)_4(THF)_{n-1}(L)$$

$$\downarrow \text{fast}$$

**products**

$$\frac{d[\text{product}]}{dt} = \frac{k_1 k_2 [L]}{k_{-1}[THF] + k_2[L]}$$

L = PPh$_3$, T = -80 °C
$k_1$ = 0.17(3) s$^{-1}$
$k_2/k_{-1}$ = 1.7(2)

strate solution was then injected into the mixing cell, and the decay of the Fe$_2$–O$_2$ intermediate followed. Product analysis was performed in independent benchtop experiments. Paddle-wheel diiron(II) complexes with sterically hindered carboxylates (dxlCO$_2^-$ family) and diiron(II) complexes with dinucleating HPTP (Scheme 2) were studied in detail.

In contrast to essentially the same kinetics of O$_2$ coordination at a vacant site,[9,10] the three dioxygen adducts, tentatively formulated as [Fe$^{III}_2$(O$_2$)(dxlCO$_2$)$_4$(L)$_2$] (L = pyridine, 1-methylimidazole, or THF), exhibited different reactivity with the substrates: only the peroxo complex for which L = THF oxidized triphenylphosphine into Ph$_3$PO at −80 °C in the absence of free dioxygen in 80% yield. The $^{18}$O label from $^{18}$O$_2$ was almost quantitatively incorporated into the phosphine oxide product. The rate of decay of the peroxo intermediate increased in the presence of Ph$_3$P by ca. 10$^4$.

Substrate coordination to one of the iron centers in [Fe$^{III}_2$(O$_2$)(dxlCO$_2$)$_4$(THF)$_2$] is necessary for productive phosphine oxidation, as the saturation kinetics suggests (Figure 6). The reaction was retarded by excess THF, confirming that phosphine oxidation is not mediated by
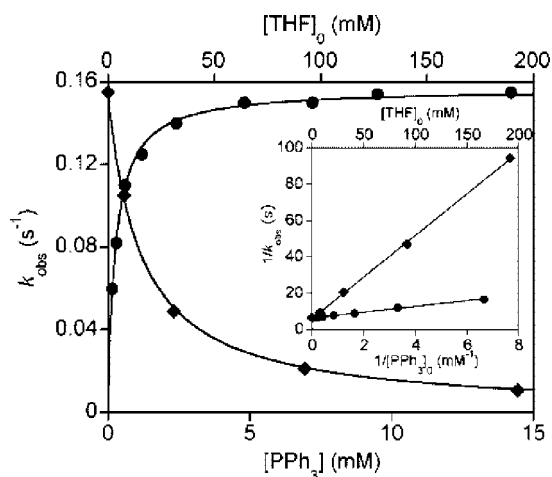


**FIGURE 6.** Plot of the pseudo-first-order rate constant $k_{obs}$ for the reaction of Fe$_2$(O$_2$)(dxlCO$_2$)$_4$(THF)$_2$ (0.3 mM) with PPh$_3$ as a function of [PPh$_3$] (●) and added [THF]$_0$ (◆) at [PPh$_3$]$_0$ = 7.5 mM and 193 K.

THF-derived radicals, and suggesting that THF dissociation is involved in the rate-limiting step. The observed first-order rate constants of intermediate decay, measured at a saturating phosphine concentration, were almost identical for a series of various para-substituted phosphines. Furthermore, the reaction of the THF-derived peroxo intermediate with pyridine or 1-methylimidazole displayed activation parameters nearly identical to those of reactions with triarylphosphines. Thus, a single-turnover oxygen atom transfer from dioxygen to PPh$_3$ was kinetically controlled by the dissociation of a monodentate THF ligand from the diiron(III)–peroxo intermediate. It can be concluded that diiron(III)–peroxo complexes with exchangeable ligands can transfer an oxygen atom to coordinating substrates that are good oxygen acceptors. Substrate coordination to one of the iron centers precedes an oxygen atom transfer.[10]

A very similar mechanism of substrate oxidation was also determined for the reactions of the diiron complex containing HPTP and bidentate bridging carboxylate, [Fe$^{III}_2$(HPTP)(O$_2$)(O$_2$CPh)]$^{2+}$.[8] In this system, only compounds capable of binding to iron (phosphines, thioanisole, and benzyl alcohol) underwent oxidation by the coordinated peroxide and displayed saturation kinetics at –40 °C in CH$_2$Cl$_2$. In contrast, noncoordinating substrates, such as 9,10-dihydroanthracene, did not react with the $\mu$-1,2-peroxo species. The bis-carboxylate [Fe$^{III}_2$(HPTP)(O$_2$)(O$_2$CPh)$_2$]$^+$, lacking open coordination sites on the iron(III) centers, does not oxidize any of the substrates mentioned above under the same conditions.

The mechanistic findings described above demonstrate the importance of ligand substitution processes in both oxygen binding to iron(II) and substrate oxidation with

diiron(III)–peroxo complexes. Dioxygen adducts of diiron(II) model complexes can oxidize strong reducing agents coordinated to one iron center. The observed greater reactivity of coordinated phosphines indirectly supports a nucleophilic nature of these deprotonated, coordinated peroxo moieties. However, our results show that even nucleophilic peroxides can transfer an oxygen atom to a closely positioned substrate. Similar "proximity effects" were reported by Lippard and co-workers for tethered substrate oxidations.[19]

## Reactions with $H_2O_2$: Peroxide Shunt Pathways

Serious problems limit applications of iron(II)–$O_2$ or diiron(II)–$O_2$ systems in catalytic oxidations, despite the appeal of $O_2$ as an oxidant. One problem appeared in the studies described above: in the absence of a proton source, diiron(III)–peroxide species can be generated rapidly at a vacant or labile iron site. However, these intermediates are nucleophilic and can transfer an oxygen atom to only good reducing agents localized in the immediate proximity of the $Fe_2(III)(O_2{}^{2-})$ moiety. Coordinated hydroperoxides are known to be electrophilic oxidants, for example, in epoxidation of electron-rich olefins. In contrast, deprotonated peroxides diplay nucleophilic reactivity and preferentially epoxidize electron-rich olefins (e.g., unsaturated ketones).[20] In the presence of a proton source during the diiron(II) oxygenation step, electrophilic activation appears to occur, but an excess of diiron(II) complex acts as a rapid and efficient reducing agent, intercepting the oxidizing equivalents and preventing external substrate oxidations. In most favorable cases, Fe(II)Fe(III) and Fe(III)Fe(IV) species result, with the latter a potentially useful one-electron oxidizing agent.[18] In most cases, various oxo-bridged diiron(III) complexes form, which no longer react with modestly reducing substrates or dioxygen. "Peroxide shunt" pathways [generating peroxo or hydroperoxo intermediates from iron(III) precursors and $H_2O_2$] may solve both problems and have proven to be successful in both heme and non-heme iron chemistry.

Hydrogen peroxide was successfully utilized in iron-catalyzed oxidations, and dinuclear catalysts sometimes outperform their mononuclear counterparts ("two irons are better than one").[2] Our interest in bimetallic oxygen activation prompted us to compare $O_2$–diiron(II) reactivity with that of analogous systems containing diiron(III) complexes and $H_2O_2$. Kinetic and mechanistic investigations of this peroxide shunt pathway are limited.[2,21]

Our detailed rapid-kinetics study of the diiron(III)–TPA complex, $[Fe^{III}_2(\mu\text{-}O)(TPA)_2(OH)(H_2O)]^{3+}$, showed stepwise formation of the previously reported diamond-core $Fe^{III}Fe^{IV}(\mu\text{-}O)_2$ complexes,[4] revealing new intermediates in this system (Scheme 11).[21] A transient diferric peroxo complex, $B_{peroxo}$ ($\lambda_{max} = 700$ nm; $\epsilon = 1500$), gradually being converted into a high-valent species, was directly observed at –40 °C in acetonitrile. The rate of formation of $B_{peroxo}$ roughly matched the rates of water substitution reactions with redox-inactive ligands, such as urea,[22,23] supporting the end-on hydroperoxo formulation. Substi-

**Scheme 11**



$$k''_{obs} = k[H_2O_2]$$
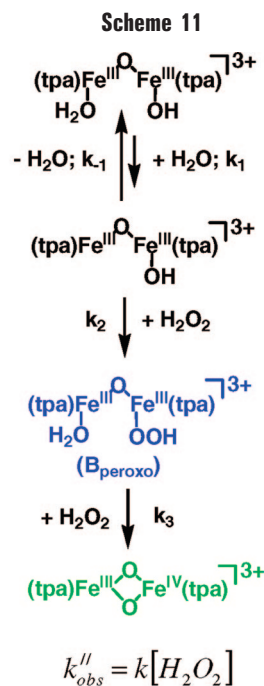
$$k'_{obs} = k_1(k_2/k_{-1})[H_2O_2]/\{(k_2/k_{-1})[H_2O_2]+[H_2O_2]\}$$

tution of the second monodentate ligand (hydroxide) into $[Fe^{III}_2(\mu\text{-}O)\text{-}(TPA)_2(OH)(H_2O)]^{3+}$ is much slower and unlikely to be involved in the reaction with $H_2O_2$. Additional spectroscopic and kinetic characterization of $B_{peroxo}$ is ongoing.

The formation of $B_{peroxo}$ from $[Fe^{III}_2(\mu\text{-}O)(TPA)_2\text{-}(OH)(H_2O)]^{3+}$ and $H_2O_2$ (characterized by the observed rate constant $k_{obs}'$) is decelerated by water and accelerated by hydrogen peroxide. Such kinetic dependence implies the existence of a steady-state intermediate between the diiron(III) precursor and $B_{peroxo}$ (Scheme 11), which forms upon loss of a water molecule from $[Fe^{III}_2(\mu\text{-}O)(TPA)_2\text{-}(OH)(H_2O)]^{3+}$.

The rate of transformation of $B_{peroxo}$ to $[Fe^{III}Fe^{IV}(\mu\text{-}O)_2(TPA)_2]^{3+}$ does not depend on $H_2O$ concentration but is proportional to $H_2O_2$ concentration (Scheme 11). Hydrogen peroxide apparently acts as a reducing agent in this reaction [the transformation of an $Fe^{III}_2(O_2)^{2-}$ species into an $Fe^{III}Fe^{IV}(O^{2-})_2$ species corresponds to a net one-electron reduction] (Scheme 11). A reductant is essential for the action of diiron enzymes (e.g., ribonucleotide reductase), presumably to reduce the $Fe^{III}_2$–peroxo intermediate to the high-valent $Fe^{III}Fe^{IV}$ intermediate.[1] The possible involvement of a second $H_2O_2$ molecule in generating high-valent diiron intermediates in enzymes and their models is commonly overlooked.

The oxidative properties of the diiron–peroxo intermediate $[Fe^{III}_2(\mu\text{-}O)(TPA)_2(OOH)(H_2O)]^{3+}$ and the high-valent complex $[Fe^{III}Fe^{IV}(\mu\text{-}O)_2(TPA)_2]^{3+}$ were studied using triphenylphosphine and 2,4-di-*tert*-butylphenol as substrates. Earlier, it was found that $[Fe^{III}Fe^{IV}(\mu\text{-}O)_2(TPA)_2]^{3+}$ oxidizes both substrates within seconds.[24,25] The reactivities of the two intermediates ($B_{peroxo}$ and $Fe^{III}Fe^{IV}$) studied by cryogenic multimixing stopped-flow experiments in our

**Scheme 12**



**Scheme 13**
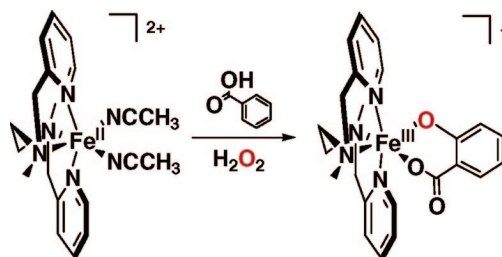


**Room Temperature, 5 min
90% yield, >90 % selectivity**
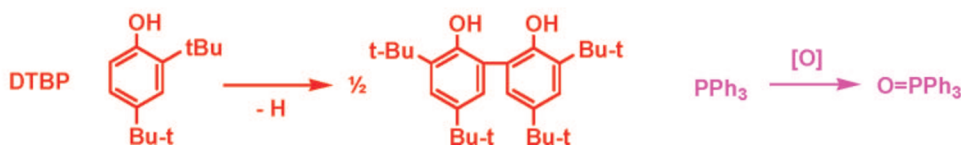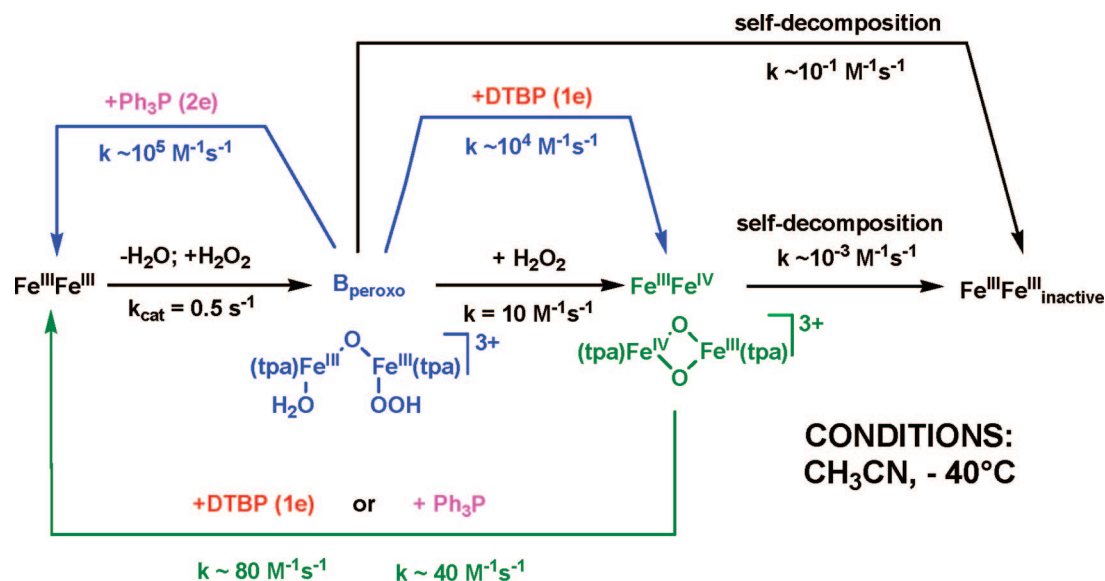
laboratories[2] were found to be very different (Scheme 12). One-electron-reducing substrate (DTBP) rapidly transformed $B_{peroxo}$ into the $Fe^{III}Fe^{IV}$ species. The reaction of $B_{peroxo}$ with $Ph_3P$ showed an even higher rate, regenerating starting diiron(III) complex in a formally two-electron process. However, when substrates were added to the high-valent Fe(III)Fe(IV) intermediate, oxidation was 2–3 orders of magnitude slower. Thus, the peroxo–diiron(III) intermediate $B_{peroxo}$ appears to be far more reactive than the high-valent $Fe^{III}Fe^{IV}$ complex (Scheme 12) and is likely involved, as a kinetically competent intermediate, in catalytic oxidations of organic substrates with $H_2O_2$ in the presence of diiron(III)–TPA complexes.[2] Ongoing mechanistic studies will uncover the role of the second iron in promoting high reactivity of $B_{peroxo}$ and related diiron–hydroperoxo intermediates. Substrate coordination at the second iron may facilitate productive (and perhaps selective) oxidations, analogous to our studies on deprotonated peroxo intermediates derived from diiron(II) and $O_2$.

## Substrate Oxidations with $H_2O_2$

Applying the principles learned from kinetic studies on oxidation of good oxygen atom acceptors (such as phosphines or phenols), we would like to eventually develop systems for oxidative catalysis (e.g., alkane or arene hydroxylation, and alkene epoxidation). Initial results for the latter two processes are already available. In diiron systems, at least one vacant or labile site must be present for $H_2O_2$ activation, and an additional vacant site(s) for substrate coordination is helpful. Monoiron complexes with one or more vacant or labile site(s) for $H_2O_2$ and substrate binding may also activate $H_2O_2$.
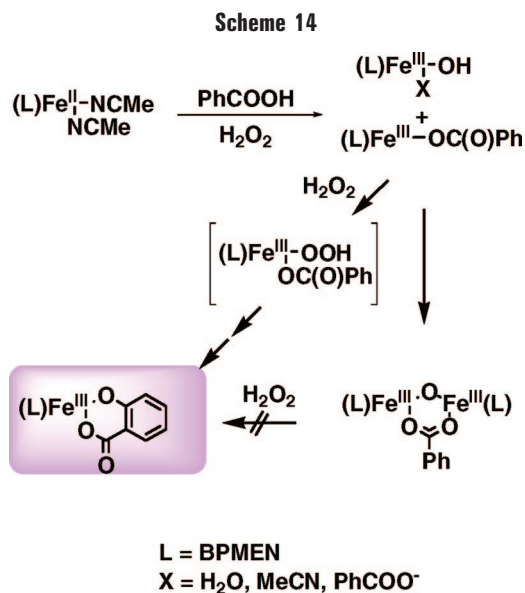
An excellent example of a $H_2O_2$-activating system is $[Fe^{II}(BPMEN)(CH_3CN)_2]^{2+}$, which efficiently catalyzes olefin epoxidation.[26,27] We have observed a new reaction promoted by this complex: stoichiometric oxidation of substituted benzoic acids into the corresponding salicylic acids with $H_2O_2$. Externally added substrates react readily under mild conditions, yielding exclusively ortho-hydroxylated products (Scheme 13).[28] Isotopic labeling proved that oxygen in the product originates from $H_2O_2$.
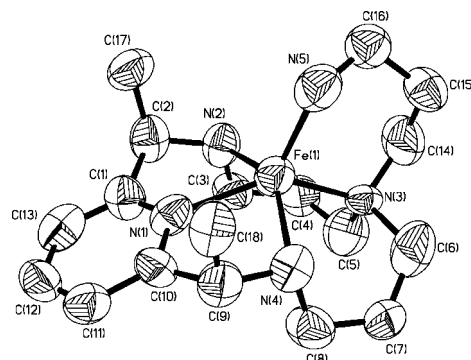
The reaction of *m*-chloroperoxybenzoic acid with [Fe(BP-MEN)]$^{2+}$ was slower and resulted in less chlorosalicylate complex compared to the analogous reaction with $m$-ClC$_6$H$_4$COOH and $H_2O_2$ (16% yield vs 74%), highlighting the importance of $H_2O_2$ and indicating that peroxybenzoate formation is not essential for hydroxylation. Preliminary results showed no H–D kinetic isotope effect in benzoic acid hydroxylation with $H_2O_2$, thus ruling out C–H bond breaking at the rate-limiting step.

**Scheme 14**



L = BPMEN

X = H₂O, MeCN, PhCOO⁻



**FIGURE 7.** ORTEP plot of [Fe(L2)]²⁺.



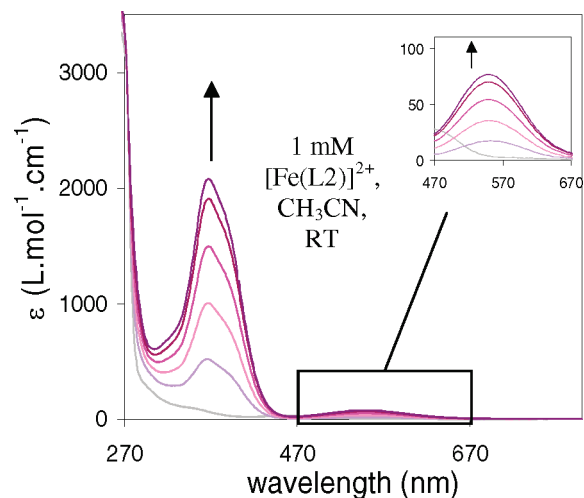**FIGURE 8.** Titration of [Fe(L2)]²⁺ with triflic acid (0–1.0 equiv).

During the first step of the reaction, benzoic acid binding and oxidation of Fe(II) into Fe(III) with $H_2O_2$ yield a mononuclear EPR-active iron(III) intermediate (Scheme 14).[28] Attempts to isolate this mononuclear, redox-active Fe(III) species led to crystallographically characterized dinuclear oxo, carboxylato-bridged [$Fe^{III}_2(\mu\text{-O})(\mu\text{-OOC-}$ $(C_6H_5))(BPMEN)_2$]³⁺, unreactive in aromatic hydroxylation.

Kinetic and spectroscopic evidence suggests that mononuclear [$Fe^{III}(BPMEN)(PhCOO)$]²⁺ further reacts with $H_2O_2$, presumably generating a short-lived hydroperoxo intermediate, which can directly attack the aromatic ring or produce high-valent iron–oxo intermediates (Scheme 14). Experimental results, however, do not exclude the possibility of formation of a dinuclear "open-core" hydroperoxo intermediate similar to $B_{peroxo}$ supported by TPA ligands (Scheme 11). Further studies of the scope and mechanism of aromatic hydroxylation are in progress.

The inability of coordinatively saturated carboxylato-bridged diiron(III) complexes of BPMEN to serve as oxidation catalysts was confirmed in an additional study of olefin epoxidation.[29] The open-core iron(III) complex [$Fe_2(\mu\text{-O})(OH)(OH_2)$ $(BPMEN)_2$]³⁺ was mildly active in epoxidation, but addition of acetic acid decreased the activity. The corresponding acetato-bridged complex [$Fe_2(\mu\text{-}$ $O)(\mu\text{-OAc})(BPMEN)_2$]³⁺, possible involvement of which in olefin epoxidation was previously debated,[26,27] was unreactive in our hands. Other coordinatively saturated complexes bearing monodentate fluoride and/or acetate anions were similarly unreactive. Although olefin sub-

strates cannot coordinate to the metal centers, the oxidant (hydrogen peroxide) certainly can, and $H_2O_2$ coordination at a vacant or labile site appears to be necessary for olefin epoxidation.[29]

To further study the mechanism of epoxidation with non-heme iron catalysts and the effects of different iron coordination spheres on catalysis, we have developed a series of macrocyclic ligands for iron (L1–L5, Scheme 2) that enforce a square-pyramidal geometry around high-spin iron(II) (Figure 7) and resemble the coordination environment in natural oxygen-activating systems such as bleomycin.[30] The large (0.6–0.7 Å) displacement of iron from the macrocyclic plane toward the coordinating appended amino group prevented binding of additional ligands in the sixth position.

The flexible aminopropyl pendant arm undergoes reversible protonation (Figure 8), liberating a coordination site for peroxide binding. Protonation of the arm, which converts the complex to a low-spin state and pseudo-

**Scheme 15**



R = H or CH₃
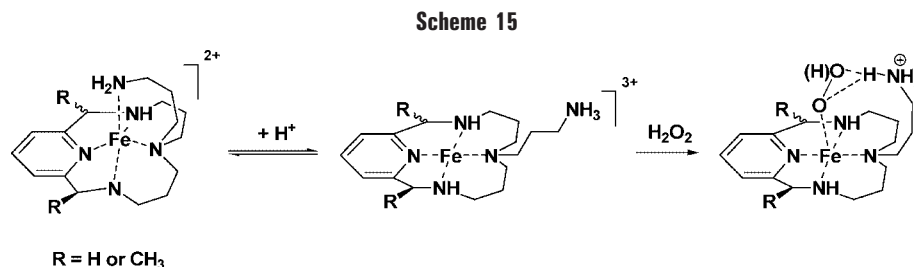
octahedral geometry (with two labile solvent molecules in the axial positions), has a profound effect on the complex reactivity. In the presence of triflic acid, these complexes efficiently and selectively catalyze cyclooctene and 1-decene epoxidation with $H_2O_2$, under mild conditions, yielding up to 90% of the products in 5 min. However, in the deprotonated form or in the presence of coordinating acids like HCl, no epoxidation occurs. Complexes with tetradentate ligands L4 and L5 catalyze olefin epoxidation to a lesser extent, and the effects of acid, attributable to electrophilic activation of coordinated peroxide via proton transfer from the pendant arm in L1–L3 (Scheme 15), are less pronounced. It follows that both the availability of a binding site for $H_2O_2$ and the presence of an intramolecular proton source improve catalytic activity of these mononuclear iron complexes.[30]

## Conclusions

Inner-sphere reactions dominate the formation and reactivity of various iron–peroxo species. Binding of dioxygen to diiron(II) complexes is an associative, low-barrier, entropically controlled process. Formation of the first iron–$O_2$ bond is rate-limiting. Therefore, oxygenation occurs rapidly at vacant or labile iron(II) sites. Oxygenation of coordinatively saturated diiron(II) complexes requires ligand dissociation. The excessive steric bulk of the multidentate ligands retards dioxygen binding. Mononuclear redox-active iron(II) complexes also provide access to the diiron(III)–peroxo species in a two-step, bimetallic reaction.

Diiron(III)–peroxo intermediates are relatively sluggish oxidants and can transfer an oxygen atom to only strong reducing agents (e.g., phosphines) coordinated to one of the irons. Similar proximity effects may account for the selectivity of enzymatic oxidations at non-heme iron centers. Electrophilic activation of diiron–peroxo species is expected to improve their ability to oxidize external electron-rich substrates. However, proton transfer in the course of $O_2$ binding is ineffective, because excess of iron(II) precursor intercepts electrophilic hydroperoxides. Delivery of a proton to preformed peroxides appears to be a promising strategy.

Reactions of diiron(III)–TPA complexes with $H_2O_2$ yielded a hydroperoxo intermediate that oxidized phosphines and phenols much faster than the Fe(III)Fe(IV) species. This is remarkable, because analogous mononuclear iron(III)–hydroperoxide complexes are believed to be poor oxidants. The role of the second iron may once again involve substrate coordination.

Although the importance of vacant sites and ligand substitution processes in facilitating redox activation of $O_2$ and $H_2O_2$ is somewhat surprising, its realization helps in designing selective oxidation catalysts and reagents. Catalytic olefin epoxidation and inner-sphere stoichiometric selective aromatic ortho hydroxylation with $H_2O_2$ were demonstrated with coordinatively unsaturated iron complexes with aminopyridine ligands.

## References

(1) Solomon, E. I.; Brunold, T. C.; Davis, M. I.; Kemsley, J. N.; Lee, S.-K.; Lehnert, N.; Neese, F.; Skulan, A. J.; Yang, Y.-S.; Zhou, J. Geometric and Electronic Structure/function Correlations in Non-heme Iron Enzymes. *Chem. Rev.* **2000**, *100*, 235–349.

(2) Kryatov, S. V.; Rybak-Akimova, E. V.; Schindler, S. Kinetics and Mechanisms of Formation and Reactivity of Non-Heme Iron Oxygen Intermediates. *Chem. Rev.* **2005**, *105*, 2175–2226.

(3) Costas, M.; Mehn, M. P.; Jensen, M. P.; Que, L., Jr. Dioxygen Activation at Mononuclear Nonheme Iron Active Sites: Enzymes, Models, and Intermediates. *Chem. Rev.* **2004**, *104*, 939–986.

(4) Que, L., Jr.; Tolman, W. B. Bis($\mu$-oxo)dimetal "Diamond" Cores in Copper and Iron Complexes Relevant to Biocatalysis. *Angew. Chem., Int. Ed.* **2002**, *41*, 1114–1137.

(5) MacMurdo, V. L.; Zheng, H.; Que, L., Jr. Model for the Cofactor Formation Reaction of *E. coli* Ribonucleotide Reductase. From a Diiron(II) Precursor to an $Fe^{III}Fe^{IV}$ Species via a Peroxo Intermediate. *Inorg. Chem.* **2000**, *39*, 2254–2255.

(6) Kryatov, S. V.; Rybak-Akimova, E. V.; MacMurdo, V. L.; Que, L., Jr. A Mechanistic Study of the Reaction between a Diiron(II) Complex $[Fe^{II}{}_2(\mu\text{-OH})_2(6\text{-Me}_3\text{-TPA})]^{2+}$ and $O_2$ to Form a Diiron(III) Peroxo Complex. *Inorg. Chem.* **2001**, *40*, 2220–2228.

(7) Kryatov, S. V.; Taktak, S.; Korendovych, I. V.; Rybak-Akimova, E. V.; Kaizer, J.; Torelli, S.; Shan, X.; Mandal, S.; MacMurdo, V. L.; Mairata i Payeras, A.; Que, L., Jr. Dioxygen Binding to Complexes with $Fe^{II}{}_2(\text{-OH})_2$ Cores: Steric Control of Activation Barriers and $O_2$-Adduct Formation. *Inorg. Chem.* **2005**, *44*, 85–99.

(8) Costas, M.; Cady, C. W.; Kryatov, S. V.; Ray, M.; Ryan, M. J.; Rybak-Akimova, E. V.; Que, L., Jr. Role of Carboxylate Bridges in Modulating Nonheme Diiron(II)/$O_2$ Reactivity. *Inorg. Chem.* **2003**, *42*, 7519–7530.

(9) Chavez, F. A.; Ho, R. Y. N.; Pink, M.; Young, V. G., Jr.; Kryatov, S. V.; Rybak-Akimova, E. V.; Andres, H.; Munck, E.; Que, L., Jr.; Tolman, W. B. Unusual Peroxo Intermediates in the Reaction of Dioxygen with Carboxylate-Bridged Diiron(II,II) Paddlewheel Complexes. *Angew. Chem., Int. Ed.* **2002**, *41*, 149–152.

(10) Kryatov, S. V.; Chavez, F. A.; Reynolds, A. M.; Rybak-Akimova, E. V.; Que, L., Jr.; Tolman, W. B. Mechanistic Studies on the Formation and Reactivity of Dioxygen Adducts of Diiron Complexes Supported by Sterically Hindered Carboxylates. *Inorg. Chem.* **2004**, *43*, 2141–2150.

(11) Korendovych, I. V.; Kryatov, S. V.; Reiff, W. M.; Rybak-Akimova, E. V. Diiron(II) $\mu$-Aqua-$\mu$-hydroxo Model for Non-Heme Iron Sites in Proteins. *Inorg. Chem.* **2005**, *44*, 8656–8658.

(12) Shan, X.; Que, L., Jr. Intermediates in the Oxygenation of a Nonheme Diiron(II) Complex, Including the First Evidence for a Bound Superoxo Species. *Proc. Natl. Acad. Sci. U.S.A.* **2005**, *102*, 5340–5345.

(13) Lee, D.; Lippard, S. J. In *Comprehensive Coordination Chemistry II*; McCleverty, J. A., Meyer, T. J., Eds.; Elsevier: Oxford, U.K., 2004; Vol. 8, pp 309–342.

(14) Zhao, M.; Song, D.; Lippard, S. J. Water Induces a Structural Conversion and Accelerates the Oxygenation of Carboxylate-Bridged Non-Heme Diiron Enzyme Synthetic. Analogues. *Inorg. Chem.* **2006**, *45*, 6323–6330.

(15) Korendovych, I. V.; Kryatova, O. P.; Reiff, W. M.; Rybak-Akimova, E. V. Iron(II) Complexes with Amide-Containing Macrocycles as Non-heme Porphyrin Analogues. *Inorg. Chem.* **2007**, *46*, 4197–4211.

(16) Korendovych, I. V.; Staples, R. J.; Reiff, W. M.; Rybak-Akimova, E. V. A New High-spin Iron(III) Complex with a Pentadentate Macrocyclic Aminopyridine Ligand: A Change from Slow Single-ion Paramagnetic Relaxation to Long-range Antiferromagnetic Order in a Hydrogen-bonded Network. *Inorg. Chem.* **2004**, *43*, 3930–3941.

(17) Murray, L. J.; Garcia-Serres, R.; Naik, S.; Huynh, B. H.; Lippard, S. J. Dioxygen Activation at Non-Heme Diiron Centers: Characterization of Intermediates in a Mutant Form of Toluene/o-Xylene Monooxygenase Hydroxylase. *J. Am. Chem. Soc.* **2006**, *128*, 7458–7459.

(18) Tshuva, E. Y.; Lippard, S. J. Synthetic Models for Non-Heme Carboxylate-Bridged Diiron Metalloproteins: Strategies and Tactics. *Chem. Rev.* **2004**, *104*, 987–1012.

(19) Yoon, S.; Lippard, S. J. Mechanistic Studies of the Oxidative N-Dealkylation of a Substrate Tethered to Carboxylate-Bridged Diiron(II) Complexes, $[Fe_2$ (mu-$O_2$CArTol)$_2$($O_2$CArTol)$_2$(N,N-Bn$_2$en)$_2$]. *Inorg. Chem.* **2006**, *45*, 5438–5446.

(20) Lane, B. S.; Burgess, K. Metal-Catalyzed Epoxidations of Alkenes with Hydrogen Peroxide. *Chem. Rev.* **2003**, *103*, 2457–2473.

(21) Kryatov, S. V.; Rybak-Akimova, E. V. A Kinetic Study of the Formation of a Model High-valent Diiron Non-heme Complex, [Fe$^{III}$Fe$^{IV}$($\mu$-O)$_2$. (tpa)2]$^{3+}$ (tpa = tris(2-pyridylmethyl)amine), by Cryogenic Stopped-flow Techniques. *J. Chem. Soc., Dalton Trans.* **1999**, 3335–3336.

(22) Kryatov, S. V.; Nazarenko, A. Y.; Robinson, P. D.; Rybak-Akimova, E. V. A Dinuclear Iron(III) Complex with a Bridging Urea Anion: Implications for the Urease Mechanism. *Chem. Commun.* **2000**, 921–922.

(23) Taktak, S.; Kryatov, S. V.; Rybak-Akimova, E. V. Reactivity of a ($\mu$-Oxo)($\mu$-hydroxo)diiron(III) Diamond Core with Water, Urea, Substituted Ureas, and Acetamide. *Inorg. Chem.* **2004**, *43*, 7196–7209.

(24) Kim, C.; Dong, Y.; Que, L., Jr. Modeling Nonheme Diiron Enzymes: Hydrocarbon Hydroxylation and Desaturation by a High-Valent Fe$_2$O$_2$ Diamond Core. *J. Am. Chem. Soc.* **1997**, *119*, 3635–3636.

(25) Leising, R. A.; Brennan, B. A.; Que, L., Jr.; Fox, B. G.; Münck, E. Models for Non-heme Iron Oxygenases: A High-valent Iron-oxo Intermediate. *J. Am. Chem. Soc.* **1991**, *113*, 3988–3990.

(26) Ryu, J. Y.; Kim, J.; Costas, M.; Chen, K.; Nam, W.; Que, L., Jr. High Conversion of Olefins to cis-Diols by Non-heme Iron Catalysts and H$_2$O$_2$. *Chem. Commun.* **2002**, 1288–1289.

(27) White, M. C.; Doyle, A. G.; Jacobsen, E. N. A Synthetically Useful, Self-Assembling MMO Mimic System for Catalytic Alkene Epoxidation with Aqueous H$_2$O$_2$. *J. Am. Chem. Soc.* **2001**, *123*, 7194–7195.

(28) Taktak, S.; Flook, M. M.; Foxman, B. M.; Que, L., Jr.; Rybak-Akimova, E. V. ortho-Hydroxylation of Benzoic Acids with Hydrogen Peroxide at a Non-heme Iron Center. *Chem. Commun.* **2005**, *42*, 5301–5303.

(29) Taktak, S.; Kryatov, S. V.; Haas, T. E.; Rybak-Akimova, E. V. Diiron(III) Oxo-bridged Complexes with BPMEN and Additional Monodentate or Bidentate Ligands: Synthesis and Reactivity in Olefin Epoxidation with H$_2$O$_2$. *J. Mol. Catal. A: Chem.* **2006**, *259*, 24–34.

(30) Taktak, S.; Ye, W.; Herrera, A. M.; Rybak-Akimova, E. V. Synthesis and catalytic Properites in Olefin Epoxidation of Novel Iron (II) Complexes with Pyridine-Containing Macrocycles Bearing on Aminopropyl Pendant Arm. *Inorg. Chem.* **2007**, *46*, 2929–2942.